International Journal of Design & Nature and Ecodynamics
Vol. 21, No. 10, October, 2026, pp. 2899-2908
Journal homepage: http://iieta.org/journals/ijdne

Evaluating Sentinel-2 Spectral Indices for Exploratory Soil pH Mapping in Dibis District, Iraq

Banaz Nadhim Jabar[1*], Qahtan A.M. Al Nuaimy[1], Yusuf Kağan Kadioğlu[2]

[1] Department of Surveying Technical Engineering, Technical Engineering College of Kirkuk, Northern Technical University, Kirkuk 36001, Iraq
[2] Department of Geological Engineering, College of Engineering, Ankara University, Ankara 06830, Turkey

Corresponding Author Email: banaz.jabar@ntu.edu.iq

Copyright: ©2026 The authors. This article is published by IIETA and is licensed under the CC BY 4.0 license (http://creativecommons.org/licenses/by/4.0/).

https://doi.org/10.18280/ijdne.211005

Received: 21 July 2026
Revised: 2 October 2026
Accepted: 14 October 2026
Available online: 31 October 2026

Keywords:
soil pH, Sentinel-2, spectral indices, linear regression, spatial mapping

ABSTRACT

The soil pH is an essential parameter that reflects nutrient availability, chemical processes, and soil fertility. Laboratory measurements are reliable methods for obtaining accurate results; however, they cannot adequately characterize the spatial distribution of the studied parameter over large areas. The aim of this research is to investigate the possibility of estimating soil pH and mapping its spatial distribution using Sentinel-2 multispectral imagery in Dibis District, Kirkuk Governorate, Iraq. Laboratory measurements of soil pH from 50 soil samples and surface reflectance data from Sentinel-2 Level-2A (L2A) imagery were used in this study. Eight spectral indices were considered: normalized difference vegetation index (NDVI), red-edge normalized difference vegetation index (NDVIre), B11/B12, B12/B11, B4/B2, B4/B3, B8/B4, and B8A/B11. Simple linear regression models were developed to investigate the relationships between the spectral indices and the laboratory-measured soil pH values. The 50 samples were randomly divided into two datasets, with 70% (35 samples) used for model development and the remaining 30% (15 samples) reserved for independent testing. Model performance was evaluated using the coefficient of determination (R^2), root mean square error (RMSE), mean absolute error (MAE), correlation coefficients, and statistical significance. The testing results indicated that B12/B11 achieved the highest correlation-based $R^2 = 0.17897$, followed by B11/B12 ($R^2 = 0.17550$). However, neither relationship was statistically significant ($p > 0.05$). When the regression equations developed using the training dataset were applied to the independent testing samples, B12/B11 achieved an RMSE of 0.11496, an MAE of 0.09782, and a predictive R^2 of 0.00588, whereas B11/B12 achieved an RMSE of 0.11603, an MAE of 0.09878, and a predictive R^2 of −0.01273. These results indicate that the evaluated spectral indices had limited predictive performance for soil pH estimation. Spatial maps were generated using a GIS environment to illustrate the exploratory distribution of soil pH estimates in the study area. The findings highlight the limitations of using individual Sentinel-2 spectral indices for soil pH prediction and emphasize the need for further validation using larger datasets.

1. INTRODUCTION

Soil pH is among the chemical soil properties that play a significant role in defining the soil environment since it affects nutrient availability, microbial activity, chemical reactions, and overall soil suitability for agricultural production [1]. Different soil pH values affect nutrient solubility and availability, thus affecting plant growth and soil fertility. Spatial distribution data concerning soil pH are therefore essential for agricultural planning and soil management. Traditional soil pH determination, however, involves sampling and laboratory measurements. Although this method is accurate enough, it may require additional time and costs when detailed information about spatial variability is needed [1]. Therefore, integrating laboratory measurements with satellite-derived information may provide a useful approach for supporting soil assessment and identifying areas that require further investigation, particularly in agricultural regions.

Remote sensing has become a promising tool that can facilitate soil property assessment because it provides spatially continuous information on the basis of satellite observations. Multispectral imaging makes it possible to analyse reflectance characteristics in the visible, near-infrared (NIR), red-edge, and shortwave-infrared (SWIR) wavelength ranges. Such regions may include features related to soil composition, surface conditions, moisture, mineral content, and vegetation cover [2-4]. Satellite missions such as Sentinel-2 are valuable for environmental and agricultural applications owing to their multispectral capability at multiple spatial resolutions. There

are many cases in which a combination of Sentinel-2 imagery, field measurements, and environmental parameters can be used for the estimation of soil pH and other soil properties [5, 6].

Several spectral indices derived from various combinations of satellite bands can be used to examine the connection between remotely sensed data and soil properties. Calculating ratios and normalized combinations of spectral bands can make differences in spectral response more apparent. On the other hand, the correlation between spectral indices and soil pH values cannot be taken for granted and is likely to vary depending on different environmental factors, such as soil moisture, land cover, soil roughness, organic content, and mineral content. For this reason, laboratory measurements need to be used to evaluate the accuracy of soil pH estimation through spectral indices rather than assumptions. Previous studies have revealed that the combination of remote sensing data and field observations facilitates the spatial assessment of soils and provides soil property maps [7, 8].

In this study, eight spectral indices were selected to represent different combinations of Sentinel-2 spectral bands and to examine their potential relationships with soil pH. These indices include normalized difference vegetation index (NDVI) and red-edge normalized difference vegetation index (NDVIre), which incorporate NIR and red-edge information; B11/B12 and B12/B11, which represent reciprocal combinations of SWIR bands; B4/B2 and B4/B3, which combine visible spectral bands; and B8/B4 and B8A/B11, which combine NIR information with visible or SWIR bands. The selection of these indices allows a comparative evaluation of different spectral responses rather than assuming that a particular index is directly or exclusively related to soil pH. Their performance is therefore examined against laboratory measurements to determine which combinations show relatively stronger relationships and whether these relationships provide useful predictive information.

Nevertheless, the performance of Sentinel-2 spectral indices for soil pH estimation needs to be evaluated under specific local environmental conditions. In Dibis District, the regional geological setting, which includes Quaternary deposits and sedimentary formations such as Injana, Mukdadiya, and Bai Hassan, provides a geological context for examining potential variations in soil properties. In addition, the relatively flat to undulating terrain may contribute to differences in drainage, sediment redistribution, and surface conditions. These factors may influence the spectral response of exposed soil and the relationship between satellite-derived indices and laboratory-measured soil pH. Furthermore, the measured soil pH values in Dibis District ranged from 7.5 to 8.2, indicating a relatively narrow range of predominantly alkaline soil conditions. This provides an opportunity to examine the sensitivity and limitations of Sentinel-2 spectral indices in detecting subtle spatial variations in soil pH under relatively uniform alkaline conditions, rather than across a broad range of acidic and alkaline soils. Therefore, the contribution of this study is not limited to testing eight spectral indices in a new geographical location; it also provides a comparative assessment of their performance under local geological and surface conditions and examines the limitations of simple linear regression for exploratory soil pH mapping. Unlike studies that evaluate soil properties across broader environmental conditions or combine multiple environmental predictors, this research focuses on comparing eight individual Sentinel-2 spectral indices using laboratory-measured soil pH and simple linear regression in a locally defined study area. This provides an assessment of the extent to which these indices can distinguish spatial variations within a relatively narrow alkaline pH range and identifies the limitations of using spectral indices alone.

From an agricultural and soil-resource management perspective, understanding the spatial variation of soil pH can help identify areas with potentially different soil conditions, support the prioritization of future soil sampling, and provide preliminary information for agricultural land assessment. Although the maps produced in this study are exploratory and do not establish reliable predictions at unsampled locations, the evaluation provides a basis for further investigation of Sentinel-2 data as a supplementary tool for soil monitoring and sustainable management of agricultural resources.

Thus, the goal of the current study is to evaluate eight Sentinel-2 spectral indices for soil pH estimation in Dibis District, Kirkuk Governorate, Iraq, on the basis of laboratory measurements of soil pH in 50 soil samples. To achieve this goal, the following tasks must be fulfilled: (i) calculation and comparison of the indices based on Sentinel-2 images; (ii) evaluation of the relationships between soil pH and the indices using simple linear regression; (iii) assessment of model performance based on statistical and error metrics; and (iv) creation of spatial distribution maps for soil pH based on the best-performing indices and regression equations using GIS technology.

2. LOCATION, MATERIALS AND GEOLOGICAL SETTING

The Kirkuk Governorate is an important administrative and economic center in northern Iraq and is located approximately 236 km north of Baghdad. The governorate is situated at approximately 35°28′ N latitude and 44°24′ E longitude. Its geographical position and natural resources contribute to its agricultural and economic importance [9, 10]. The present study focuses on Dibis District, which is located in the northwestern part of Kirkuk Governorate. Dibis includes a variety of landscape settings, ranging from relatively flat areas to undulating terrain, which may influence soil formation, drainage, and the spatial distribution of soil properties. The location and boundaries of the study area are presented in Figure 1.

Field sampling was conducted on 1 August 2026, and 50 soil samples were collected from locations distributed across Dibis District. These samples were used to investigate the spatial variability of soil pH. The Sentinel-2 Level-2A (L2A) imagery acquired on 5 August 2026 was used as the satellite data source. This product provides bottom-of-atmosphere (BOA) surface reflectance following atmospheric correction, supporting the investigation of spectral characteristics associated with soil properties. Previous studies have demonstrated the potential of integrating satellite observations with field and laboratory measurements for soil pH estimation and spatial mapping [7, 8, 11].

Geologically, Kirkuk Governorate lies within the Foothill Zone and the low-folded domain of the Zagros Fold–Thrust Belt in northeastern Iraq. Regional compressional tectonic forces have contributed to the development of anticlines and synclines, many of which generally trend northwest–southeast. These structures influence the distribution and exposure of sedimentary formations across the region [12, 13]. The regional geomorphology is characterized by folded hills,

dissected terrain, valleys, and relatively flat areas associated with alluvial deposition. These landforms reflect the combined effects of tectonic development, erosion, and fluvial processes, which influence sediment transport and the redistribution of surface materials [14]. The principal geological units and their spatial distribution within Kirkuk Governorate are illustrated in Figure 2.

The regional stratigraphy includes Quaternary deposits, such as alluvium, floodplain sediments, and slope-derived materials, which may contribute to the parent materials of local soils [10, 15]. Older sedimentary formations are exposed in elevated areas and along fold structures. These include the late Miocene Injana Formation, consisting of alternating sandstone, siltstone, and claystone; the Mukdadiya Formation, characterized by sandstone, gravel, and clay-rich deposits; and the Bai Hassan Formation, which contains coarse clastic sediments and conglomerates [12, 16, 17].

Weathering of these sedimentary rocks, together with erosion and deposition, may influence soil texture, mineral composition, and chemical characteristics. Differences in parent materials, drainage conditions, and topographic position may therefore contribute to soil pH variability across Dibis District. These geological and geomorphological characteristics provide the regional context for examining local soil pH variations and their spatial representation using Sentinel-2 imagery and GIS techniques.

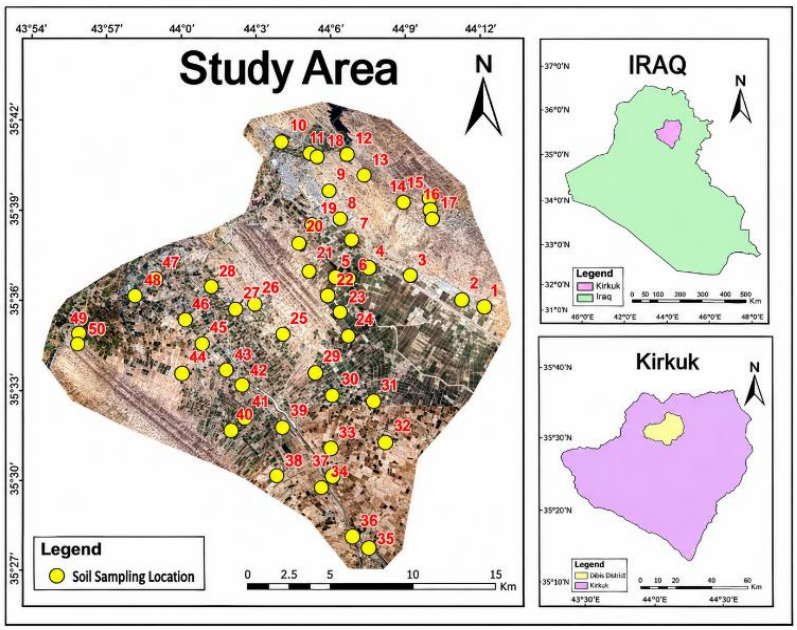

Figure 1. Location of the study area and spatial distribution of soil sampling sites in Dibis District, Kirkuk Governorate, Iraq

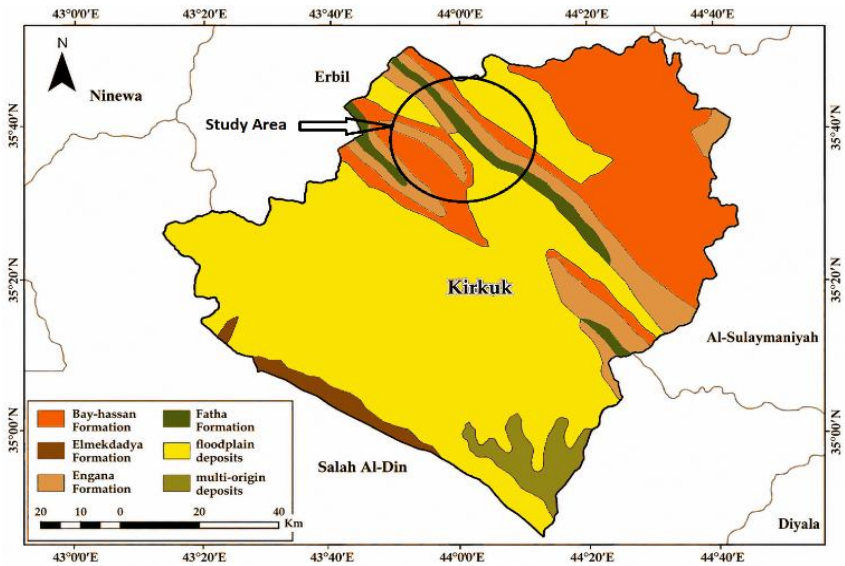

Figure 2. Geological map of the study area in Kirkuk, illustrating the various stratigraphic formations and structural features of the region

Note: Modified from study [17].

3. METHODOLOGY

In the present research, laboratory-based soil pH measurements together with Sentinel-2 L2A imagery were used to evaluate the possibility of estimating soil pH on the basis of spectral indices in Dibis District, Kirkuk, Iraq. Specifically, 50 soil samples collected on 1 August 2026 were used, along with a single Sentinel-2 L2A image acquired on 5

August 2026. The atmospherically corrected Sentinel-2 L2A image was selected and downloaded based on its low cloud coverage over the study area. Soil sampling locations were selected to ensure geographical coverage of the study area. The Sentinel-2A L2A BOA surface reflectance product was acquired at 07:50:21 UTC, with tile identifier T38SME and processing baseline 05.12. The product identifier was S2A_MSIL2A_20260805T075021_N0512_R135_T38SME_20260805T131115.SAFE. The image was selected based on its low cloud coverage over the study area, and no additional cloud-masking procedure was applied. The spectral bands originally available at 20 m spatial resolution were resampled to 10 m to ensure spatial consistency among the bands used in the analysis. The spectral indices were calculated using the BOA surface reflectance values provided in the Sentinel-2 L2A product. No additional reflectance calibration or scaling was applied beyond the product-provided values. Because all evaluated indices were based on ratios of spectral bands, any uniform multiplicative scaling factor applied consistently to the reflectance values would cancel out during index calculation and would therefore not affect the resulting index values. The NDVIre was calculated using NIR Band 8A and red-edge Band 5, according to the following equation:

$$NDVIre = \frac{B8A - B5}{B8A + B5}$$

Table 1. Soil sampling locations and measured pH values in Dibis District, Kirkuk, Iraq

Sample ID	Easting (m)	Northing (m)	Soil pH	Dataset Assignment
1	427927	3939760	7.8	Training
2	426573	3940181	7.5	Training
3	423425	3941649	7.7	Training
4	420935	3942177	7.7	Training
5	418875	3941580	8.0	Training
6	419722	3941448	7.7	Training
7	419950	3943876	7.7	Test
8	419198	3945156	7.6	Training
9	418522	3946886	7.7	Training
10	415648	3949893	8.1	Test
11	417369	3949197	7.7	Training
12	419609	3949109	8.1	Training
13	420654	3947820	8.1	Test
14	423085	3946167	8.0	Test
15	424647	3946403	8.1	Training
16	424727	3945733	8.2	Training
17	424845	3945157	8.1	Training
18	417808	3949005	7.8	Test
19	417497	3944818	8.1	Test
20	416675	3943640	8.2	Training
21	417305	3941928	7.8	Test
22	418384	3940475	8.0	Training
23	419171	3939411	7.9	Test
24	419679	3937901	7.8	Training
25	415722	3938078	7.9	Test
26	414026	3939930	8.0	Training
27	412875	3939613	7.9	Training
28	411370	3940956	7.7	Training
29	417693	3935754	7.8	Training
30	418672	3934330	7.8	Test
31	421197	3933968	7.8	Training
32	421917	3931464	7.8	Training
33	418613	3931062	7.9	Test
34	418711	3929365	7.8	Test
35	420929	3924928	7.8	Test
36	419941	3925629	7.8	Training
37	418034	3928661	7.9	Training
38	415325	3929363	7.8	Training
39	415697	3932368	7.8	Training
40	412530	3932210	7.9	Training
41	413349	3932959	7.9	Training
42	413240	3934988	8.1	Training
43	412259	3935902	7.9	Training
44	409606	3935724	7.8	Test
45	410801	3937512	7.7	Training
46	409771	3938941	7.8	Training
47	407955	3941469	7.7	Training
48	406754	3940419	7.8	Training
49	403314	3938112	7.9	Training
50	403281	3937489	7.9	Test

Spectral values for the eight evaluated indices were extracted at the 50 soil sampling locations using the Extract Multi Values to Points tool in ArcGIS. No additional vegetation mask or NDVI-based threshold was applied because vegetation cover in the study area was limited. The 50 soil samples were collected at a depth of 30–40 cm. Before laboratory analysis, the samples were dried and sieved. Soil pH was measured using a soil-to-water suspension ratio of 1:2.5 (weight:volume), prepared by adding 30 g of soil to 75 mL of distilled water. The mixture was shaken and allowed to settle, and the pH was measured in the clear supernatant using a pH meter at room temperature. Measurements were repeated to ensure the consistency of the results.

Eight spectral indices were calculated and analysed through simple linear regression to determine their relationships with soil pH. The 50 samples were randomly divided into two subsets, with 35 samples (70%) assigned to the training dataset for model development and 15 samples (30%) assigned to the testing dataset for independent evaluation. The sample identifiers and their respective dataset assignments are provided in Table 1.

The regression coefficients (intercept and slope) for each spectral index were estimated exclusively using the 35 training samples. The resulting regression equations were then applied directly to the 15 testing samples to calculate predicted soil pH values. No regression refitting or coefficient adjustment was performed using the testing dataset. Therefore, the testing samples were used exclusively for independent model evaluation and calculation of predictive performance metrics.

To further assess model stability and reduce the influence of a single random data split, 500 repeated random 70/30 data splits were performed. For each repetition, the dataset was randomly divided into training and testing subsets. Regression models were developed using the training subset and subsequently evaluated using the corresponding testing subset. A baseline model was also established independently for each repetition using the mean soil pH of the training subset to predict the soil pH values of all samples in the corresponding testing subset. The percentage improvement in root mean square error (RMSE) achieved by each spectral-index model relative to the baseline model was calculated using the following equation:

$$\text{Improvement (\%)} = \frac{RMSE_{baseline} - RMSE_{index}}{RMSE_{baseline}} \times 100$$

where, RMSE baseline represents the RMSE of the baseline model, which predicts the mean soil pH of the training subset for all samples in the corresponding testing subset, and RMSE index represents the RMSE of the spectral-index regression model evaluated on the same testing subset. Positive improvement values indicate lower RMSE than the baseline model, whereas negative values indicate higher RMSE. The mean RMSE, standard deviation of RMSE, and mean percentage improvement were calculated across the 500 repetitions. The entire research workflow is schematically illustrated in Figure 3.

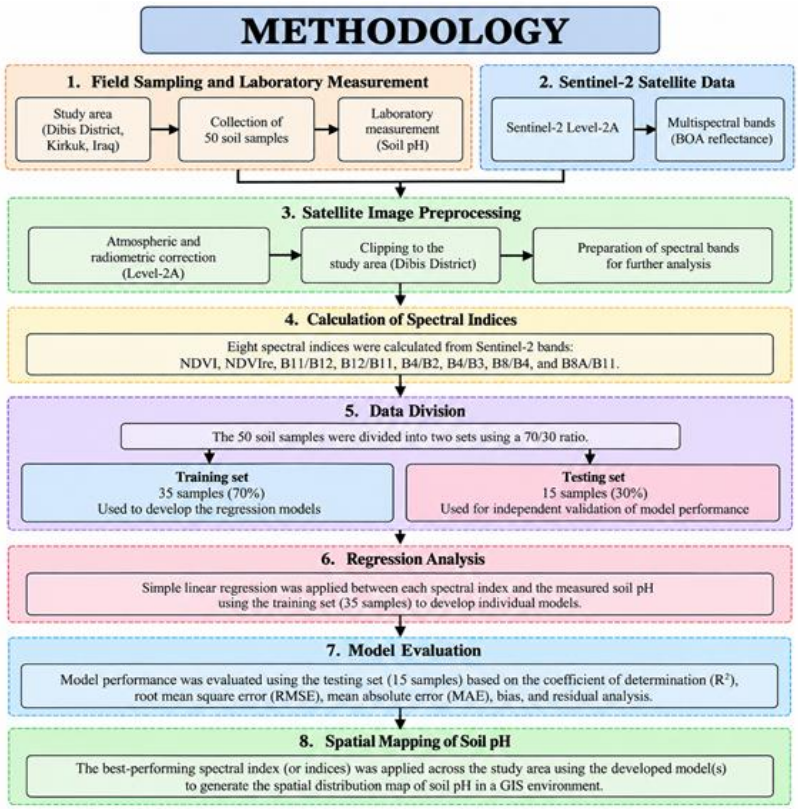

Figure 3. Methodological workflow for soil pH estimation and spatial mapping using Sentinel-2 spectral indices in Dibis District, Kirkuk, Iraq

4. RESULTS

Differences were observed in the relationships between the eight Sentinel-2 spectral indices and experimentally determined soil pH values in Dibis District, Kirkuk, Iraq. The evaluated indices included NDVI, NDVIre, B11/B12,

B12/B11, B4/B2, B4/B3, B8/B4, and B8A/B11. As shown in Table 2, the independent testing results (n = 15) indicated that B12/B11 achieved the highest predictive coefficient of determination (R^2) of 0.00588, followed by B11/B12 with a predictive R^2 of −0.01273. The predictive R^2 values of the remaining indices were negative, ranging from −0.02533 for NDVI to −0.26234 for B4/B3. These results indicate that the regression models had limited predictive performance when applied to the independent testing dataset.

The relationships between B11/B12 and B12/B11 and the measured soil pH values are illustrated in Figure 4. For B11/B12, a positive relationship was observed (r = 0.4189, p = 0.1201), whereas B12/B11 showed a negative relationship (r = −0.4231, p = 0.1161). The corresponding correlation-based R^2 were 0.17550 for B11/B12 and 0.17897 for B12/B11, respectively. These values represent the squared correlation coefficients calculated from the independent testing dataset and are distinct from the predictive R^2 values reported in Table 2. These opposite correlation directions are consistent with the reciprocal nature of the two band ratios. However, neither relationship was statistically significant at the 0.05 level. The results therefore indicate that the two indices showed relatively stronger associations with soil pH than the other evaluated indices, although their explanatory strength remained limited.

To ensure consistency between the two reciprocal SWIR band ratios, Figure 4(a) and 4(b) were generated using the same 15 independent testing samples. For each sample, B11/B12 and B12/B11 were calculated from the same Sentinel-2 spectral-band observations. These indices are mathematically reciprocal, such that (B11/B12) × (B12/B11) = 1. For example, Sample 10 had a B11/B12 value of 1.168006 and a corresponding B12/B11 value of 0.85616, whose product is approximately 1. The complete sample-level values are provided in Table 3.

Table 2. Statistical performance of eight Sentinel-2 spectral indices for soil pH estimation

Spectral Index	n	Training Slope	Test r	Test p-Value	Test RMSE	Test MAE	Predictive R^2
B11/B12	15	0.903838	0.4189	0.1201	0.11603	0.09878	−0.01273
NDVI	15	1.381530	0.2814	0.3096	0.11675	0.08899	−0.02533
NDVIre	15	1.147557	0.2394	0.3901	0.11842	0.08793	−0.05490
B12/B11	15	−1.208966	−0.4231	0.1161	0.11496	0.09782	0.00588
B4/B2	15	0.564526	−0.0672	0.8120	0.12858	0.10009	−0.24371
B4/B3	15	1.253596	0.0517	0.8547	0.12954	0.10496	−0.26234
B8/B4	15	0.522636	0.2778	0.3161	0.11699	0.08839	−0.02950
B8A/B11	15	0.685554	0.1669	0.5522	0.11951	0.09215	−0.07435

Note: Regression slopes were obtained from the training dataset (n = 35), whereas correlation coefficients (r) and p-values were calculated using the independent testing dataset (n = 15). Root mean square error (RMSE), mean absolute error (MAE), and predictive coefficient of determination (R^2) were calculated by applying the training-derived regression equations to the testing dataset without refitting. Normalized difference vegetation index (NDVI); red-edge normalized difference vegetation index (NDVIre).

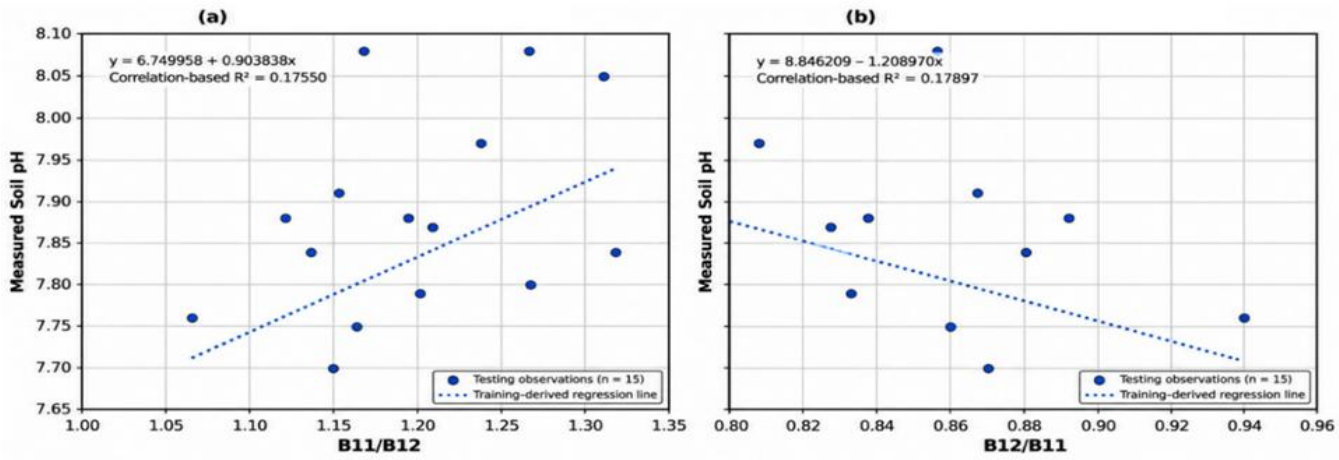

Figure 4. Relationships between Sentinel-2 spectral indices and laboratory-measured soil pH: (a) B11/B12 and (b) B12/B11

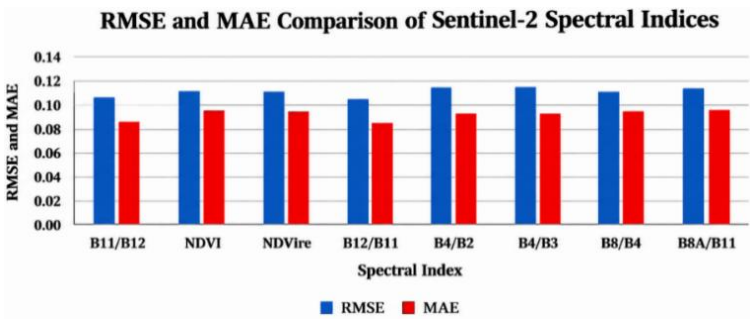

Figure 5. Comparison of the root mean square error (RMSE) and mean absolute error (MAE) values for the eight Sentinel-2 spectral indices used for soil pH estimation

Table 2 and Figure 5 present the error-based comparison of the eight indices. B12/B11 produced the lowest RMSE (0.11496), followed by B11/B12 (0.11603). The lowest mean absolute error (MAE) was obtained for NDVIre (0.08793), followed by NDVI (0.08899). In contrast, B4/B3 recorded the highest RMSE (0.12954) and MAE (0.10496). The error values indicate differences in the predictive performance of the evaluated indices; however, the generally limited predictive R^2 values show that none of the indices provided a strong prediction of soil pH in the independent testing dataset.

Table 3. Measured soil pH and reciprocal Sentinel-2 shortwave-infrared (SWIR) band ratios for the 15 independent testing samples

Sample ID	Measured pH	B11/B12	B12/B11
10	8.08	1.168006	0.85616
18	7.84	1.135768	0.880462
13	8.08	1.267074	0.78922
7	7.7	1.149319	0.870081
14	7.97	1.237533	0.808059
19	8.05	1.311376	0.762558
21	7.84	1.317664	0.758919
23	7.87	1.208631	0.827382
25	7.88	1.121355	0.891778
50	7.91	1.152951	0.867339
30	7.75	1.163209	0.85969
44	7.8	1.267356	0.789044
33	7.88	1.193822	0.837646
34	7.79	1.200948	0.832676
35	7.76	1.064687	0.939243

Note: The two indices are reciprocal ratios calculated from the same spectral-band values for each testing sample. Minor deviations from exactly 1 in their product are attributable to numerical rounding.

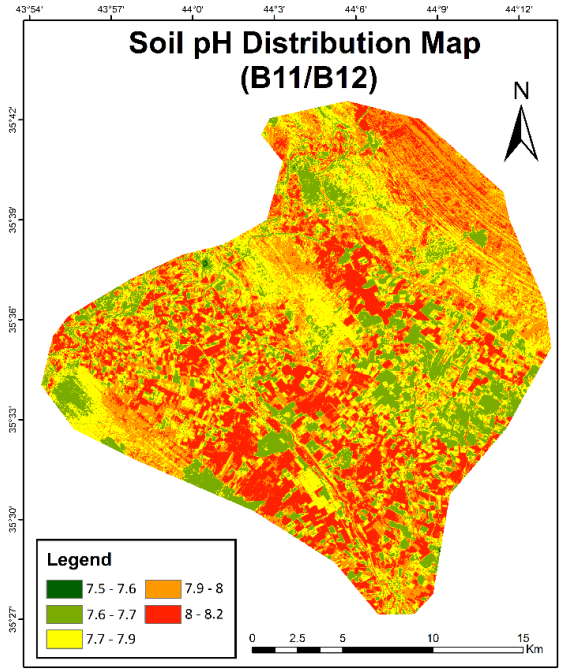

Figure 6. Spatial distribution of estimated soil pH derived from the B11/B12 spectral index in Dibis District, Kirkuk, Iraq

Based on the relative correlation results of B11/B12 and B12/B11, these two indices were selected for spatial visualization of soil pH in the study area. The soil pH map generated using B11/B12 is presented in Figure 6, whereas the map generated using B12/B11 is presented in Figure 7. These maps illustrate the spatial patterns estimated by the two indices. Since the indices are reciprocal ratios derived from the same spectral bands, their spatial patterns should be interpreted in relation to their respective relationships with measured soil pH and the limited predictive performance observed during independent testing.

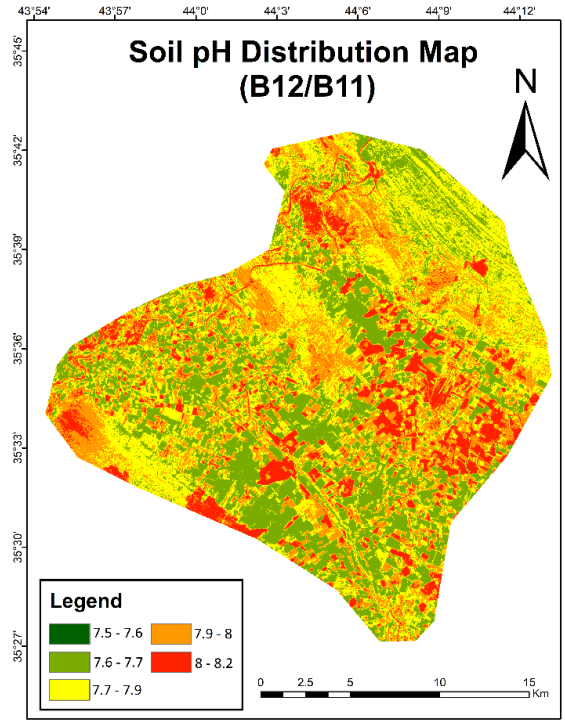

Figure 7. Spatial distribution of estimated soil pH derived from the B12/B11 spectral index in Dibis District, Kirkuk, Iraq

Furthermore, model stability was assessed through 500 repeated random 70/30 data splits, and the results are presented in Table 4. B11/B12 achieved the lowest mean RMSE (0.1493) and the greatest mean improvement over the baseline (6.10%), followed by B12/B11, with a mean RMSE of 0.1508 and a mean improvement of 5.16%. NDVI also showed a positive mean improvement of 2.30%. In contrast, NDVIre and B4/B2 recorded negative mean improvements of −0.84% and −0.92%, respectively. These findings indicate that B11/B12 and B12/B11 maintained relatively better performance across repeated random data splits compared with the baseline model, although the improvements were generally modest.

Table 4. Model performance and improvement over the baseline using 500 repeated random 70/30 data splits

Index	Mean RMSE	Standard Deviation	Mean Improvement over Baseline
B11/B12	0.1493	0.0214	6.10%
NDVI	0.1553	0.0203	2.30%
NDVIre	0.1603	0.0221	−0.84%
B12/B11	0.1508	0.0212	5.16%
B4/B2	0.1604	0.0221	−0.92%
B4/B3	0.1581	0.0214	0.44%
B8/B4	0.1559	0.0203	1.90%
B8A/B11	0.1587	0.0212	0.24%

Note: Root mean square error (RMSE), normalized difference vegetation index (NDVI), red-edge normalized difference vegetation index (NDVIre).

Overall, the results indicate that B11/B12 and B12/B11 showed relatively stronger correlations with soil pH than the other evaluated indices. Nevertheless, the independent testing results revealed limited predictive performance, as reflected by the low or negative predictive R^2 values and the absence of statistically significant correlations. The repeated-splitting analysis further supported the relative performance of these two indices, although their improvements over the baseline remained modest. Therefore, the generated maps should be considered exploratory representations of potential spatial soil pH variation rather than highly accurate predictions. Further validation using larger datasets and additional study areas is required to assess the reliability of these spectral indices.

5. DISCUSSION

As seen from the results obtained in this research, the correlation between Sentinel-2 spectral indices and soil pH changes depending on the spectral bands used in the creation of each particular index. Among all eight indices, the ratios of the SWIR bands (B11/B12 and B12/B11) showed the strongest correlations with soil pH in the independent testing dataset, with correlation coefficients of $r = 0.4189$ and $r = -0.4231$, respectively. Their corresponding correlation-based R^2 values were 0.1755 and 0.1790. However, neither relationship was statistically significant ($p > 0.05$). Furthermore, the independent predictive R^2 values were −0.01273 and 0.00588, respectively, indicating limited predictive performance. The results indicate that the information obtained from the SWIR bands of Sentinel-2 is more related to the soil pH than to the vegetation and visible-to-NIR ratios. Nevertheless, the relatively low correlation-based R^2 values and the limited predictive performance indicate a weak relationship between the indices and the soil pH.

The relatively stronger correlations of the SWIR ratios might be linked to the sensitivity of SWIR reflectance to surface properties related to soil composition, moisture status, and mineralogy. Soil pH is not assessed through satellite reflectance; instead, the estimation of soil pH from optical images is based on the relationships between soil pH and other soil and surface properties. As a result, the strength of the relationship might differ depending on the soil type, surface status, land use, and local environment. Zhang et al. [8] studied the use of Landsat 8, Sentinel-2, and Gaofen-2 imagery for the mapping of soil pH, showing how important it is to consider various sources of satellite data for this task. Similarly, the study [6] used Sentinel-2 imagery along with soil physical properties and elevation data and reported that environmental variables are essential for soil pH estimation. Both works highlight the potential usefulness of spectral indices for soil pH mapping; however, their predictive performance depends on the characteristics of the study area and the variables included in the model.

The opposite trends of B11/B12 and B12/B11 are expected because they are reciprocal band ratios derived from the same two Sentinel-2 SWIR bands. While B11/B12 showed a positive relationship with soil pH, B12/B11 showed a negative relationship. Although these indices contain the same underlying spectral information, their reciprocal mathematical transformations produce different predictor values. When simple linear regression is independently fitted to each ratio, the resulting regression coefficients and predicted soil pH values are not mathematically equivalent. Consequently, applying the two regression equations to the corresponding spectral ratios can produce different spatial patterns in the resulting maps. These differences reflect the mathematical transformation and the separately fitted regression relationships rather than independent spectral information or different soil processes. Similar correlation-based R^2 values and relatively close RMSE values for both indices reflect their shared spectral information. Nevertheless, their independent predictive R^2 values were close to zero, indicating that neither ratio provided strong predictive performance. The small numerical differences in RMSE and MAE should therefore not be interpreted as evidence of a clear predictive advantage of either index.

Moreover, the rather low correlations found here might be connected to the complicated nature of soil pH variation. The soil pH is determined by different interacting elements, such as parent material, weathering, drainage, vegetation, agricultural practices, and the transport of soluble compounds in the soil profile. In turn, satellite reflectance mostly reflects the spectral response at the surface, which can be influenced by factors such as vegetation cover, surface moisture, soil roughness, and the presence of a mixed landscape in a single pixel. Therefore, the differences in the processes determining the soil pH level and in the processes determining the spectral responses may partially explain the lack of a significant influence of the indices used in this study on the variability of the pH level in Dibis District. Charishma et al. [5] studied the relationships between Sentinel-2 imagery and soil properties and reported that the relationships differed for various properties and spectral variables.

Maps of the B11/B12 and B12/B11 ratios offer an approach for exploring the spatial distribution of soil pH within the Dibis District. However, these maps need to be interpreted in the context of the statistical limitations of the two ratios, since they are reciprocal transformations of the same spectral bands. The differences between their spatial patterns result from the different mathematical forms of the ratios and their independently fitted regression equations, rather than from independent spectral observations. Therefore, the two maps should be regarded as alternative representations of the same spectral information, not as independent mapping solutions. The maps should be considered preliminary estimates based on the developed models and interpreted cautiously in view of the limited predictive performance observed in the independent testing dataset. They should not be regarded as highly accurate representations of soil pH.

These results are in line with other advances in the field of soil mapping using remote sensing, where spectral data are becoming increasingly integrated with ground measurements and other environmental parameters. The possibility of combining remote sensing data with additional information to facilitate soil texture and pH mapping was shown by the study [7]. In a more recent study, Abdullah et al. [6] proved that the inclusion of soil physical characteristics and elevation data with Sentinel-2 spectral characteristics facilitates high-resolution soil pH mapping. Future research in the district of Dibis could explore the potential use of terrain characteristics, land cover, soil texture, and multitemporal images in addition to spectral indices. Different regression models could also be tested to determine whether correlations with spectral indices can be increased.

Another thing that needs to be kept in mind is distinguishing between model fitting and model validation. While the RMSE

and MAE are useful ways of summarizing differences in predictions, they can determine only the independent predictive capability if the data used for validation are not involved in deriving the predictive equations. In the present study, the 50 soil samples were randomly divided into 35 training samples and 15 testing samples. The regression equations were developed using only the training dataset and subsequently applied to the testing dataset without refitting. Accordingly, RMSE, MAE, and predictive R^2 were calculated from the predictions obtained for the 15 independent testing samples. Correlation coefficients and their corresponding p-values were also evaluated using the testing samples. The results showed that none of the eight indices had a statistically significant correlation with soil pH at the 0.05 level. A distinction between model-development data sets and test data sets is thus necessary for interpretation of the reported results. In future studies, this distinction must be maintained, and when possible, spatial independence or cross-validation should be used to evaluate the prediction capability [18-20].

To further assess the predictive performance of the evaluated indices, their results were compared with a baseline model that used the mean soil pH of the training dataset to predict the pH values of all testing samples. The training-set mean was 7.84, producing a baseline RMSE of 0.12204 and an MAE of 0.09333. The baseline bias, calculated as predicted minus measured pH, was −0.04000. Among the evaluated indices, B12/B11 achieved the largest reduction in RMSE (5.80%) compared with the baseline, followed by B11/B12 (4.92%). However, B4/B2 and B4/B3 produced higher RMSE values than the baseline, indicating poorer predictive performance. The bias values for B12/B11 and B11/B12 were −0.04693 and −0.04787, respectively, showing a slight underestimation of soil pH in the testing dataset.

Furthermore, 500 repeated random 70/30 data splits were conducted to examine the stability of the regression models. The results showed that B11/B12 achieved the greatest mean improvement in RMSE over the corresponding baseline (6.10%), followed by B12/B11 (5.16%). NDVI also showed a positive mean improvement of 2.30%, while B8/B4, B4/B3, and B8A/B11 showed improvements of 1.90%, 0.44%, and 0.24%, respectively. In contrast, NDVIre and B4/B2 showed negative mean improvements of −0.84% and −0.92%, respectively, indicating slightly poorer performance than the baseline. These findings suggest that B11/B12 and B12/B11 maintained relatively better performance across repeated random data splits, although the improvements were generally modest. The standard deviations of RMSE also indicated variability in model performance across the repeated splits.

The relatively low absolute RMSE values should also be interpreted in relation to the narrow measured soil pH range of 7.5–8.2. Under such a limited range, small absolute prediction errors do not necessarily indicate strong explanatory or predictive capability. Furthermore, the highest correlation-based R^2 value was approximately 0.18, indicating that the evaluated spectral indices explained only a small proportion of the observed variation in soil pH. The concentration of measured pH values within a relatively narrow alkaline range may have limited the ability of the regression models to capture stronger relationships and restricted the general applicability of the developed equations to soils with different pH conditions. This limitation is also supported by the near-zero predictive R^2 values obtained from the independent testing dataset. Therefore, the proposed Sentinel-2 spectral-index approach should be considered a preliminary method for exploring potential spatial variations in soil pH within the sampled area and under the observed soil conditions, rather than a reliable predictive model. Its applicability to other geographical areas, wider pH ranges, and unsampled soil conditions remains unconfirmed. Therefore, comparison with the training-mean baseline provides a more meaningful assessment of the practical contribution of the spectral indices.

Overall, this study represents an initial attempt to compare eight spectral indices derived from Sentinel-2 satellite imagery to investigate soil pH variations in Dibis District. Compared with the other evaluated indices, B11/B12 and B12/B11 exhibited relatively stronger correlations with laboratory measurements and were consequently used to generate exploratory soil pH maps. However, because these two indices are reciprocal transformations of the same spectral bands, their results do not represent independent spectral evidence. Furthermore, their small differences in error metrics do not establish a clear advantage for either index. Their independent predictive performance remained limited, and neither index showed a statistically significant relationship with soil pH. The low explanatory power indicates that these spectral indices alone cannot adequately account for soil pH variability in the study area.

6. CONCLUSIONS

In this research, eight Sentinel-2 spectral indices were used to evaluate their relationships with laboratory-measured soil pH and explore its spatial distribution in the district of Dibis in Kirkuk governorate, Iraq. The results revealed differences in the strength and direction of the relationships between the evaluated spectral indices and measured soil pH. Among all the tested indices, B11/B12 and B12/B11 showed relatively stronger correlations with soil pH, with correlation-based R^2 values of 0.17550 and 0.17897, respectively. In addition, B12/B11 had the lowest RMSE (0.11496) and MAE (0.09782), followed by B11/B12, with an RMSE of 0.11603 and an MAE of 0.09878 in the independent testing dataset. However, neither of these correlations was statistically significant at the 0.05 level, and their predictive R^2 values were −0.01273 for B11/B12 and 0.00588 for B12/B11, indicating limited predictive capability.

Soil pH maps were prepared with the help of B11/B12 and B12/B11 to depict the estimated soil pH distribution in the region. However, the independent testing results indicated limited predictive performance, with predictive R^2 values close to zero or negative. Furthermore, baseline comparisons and 500 repeated random data splits showed that the improvements achieved by these indices were modest. These findings suggest that Sentinel-2 spectral indices may provide exploratory information about spatial soil pH variation in Dibis District; nevertheless, their limited explanatory and predictive performance does not support their use as reliable standalone prediction models. Many factors could affect soil pH and may not be captured by these spectral ratios alone.

The generated maps should therefore be interpreted as exploratory representations of potential soil pH variation within the sampled area of Dibis District, based on the Sentinel-2 image acquired on 5 August 2026 and the observed laboratory soil pH range of 7.5–8.2. They should not be considered reliable predictions at unsampled locations or applied beyond the sampled soil conditions without further validation.

Future research could investigate the integration of Sentinel-2 spectral indices with additional environmental variables, such as soil type, topographic characteristics, and land-cover properties, as well as the use of multi-temporal satellite imagery. Moreover, additional validation with larger independent soil datasets, different sampling dates, and other geographical areas, including independent spatial validation, could help to confirm the reliability and validity of the soil pH maps generated during this research. Such validation is necessary before these maps can be used to support practical soil management decisions. Overall, this research provides an initial assessment of the potential application of Sentinel-2 spectral indices for exploring soil pH variation. The B11/B12 and B12/B11 ratios may be considered candidates for further investigation, rather than established predictive indices, under different soil and environmental conditions.

REFERENCES

[1] Xiao, S.C., Ou, M.H., Geng, Y.J., Zhou, T. (2023). Mapping soil pH levels across Europe: An analysis of LUCAS topsoil data using random forest kriging (RFK). Soil Use and Management, 39(2): 900-916. https://doi.org/10.1111/sum.12874

[2] Vaudour, E., Gomez, C., Fouad, Y., Lagacherie, P. (2019). Sentinel-2 image capacities to predict common topsoil properties of temperate and Mediterranean agroecosystems. Remote Sensing of Environment, 223: 21-33. https://doi.org/10.1016/j.rse.2019.01.006

[3] Gholizadeh, A., Žižala, D., Saberioon, M., Borůvka, L. (2018). Soil organic carbon and texture retrieving and mapping using proximal, airborne and Sentinel-2 spectral imaging. Remote Sensing of Environment, 218: 89-103. https://doi.org/10.1016/j.rse.2018.09.015

[4] Angelopoulou, T., Tziolas, N., Balafoutis, A., Zalidis, G., Bochtis, D. (2019). Remote sensing techniques for soil organic carbon estimation: A review. Remote Sensing, 11(6): 676. https://doi.org/10.3390/rs11060676

[5] Charishma, D.S., Kuligod, V.B., Gundlur, S.S., Potdar, M.P., Doddamani, M.B., Nagaveni, H.C. (2025). Estimation of top soil properties by Sentinel-2 imaging. Geology, Ecology, and Landscapes, 9(4): 1258-1267. https://doi.org/10.1080/24749508.2024.2392920

[6] Abdullah, H., Skidmore, A.K., Siegenthaler, A., Neinavaz, E. (2025). High-resolution prediction of soil pH in European temperate forests using Sentinel-2 and ancillary environmental data. Scientific Reports, 15(1): 28509. https://doi.org/10.1038/s41598-025-03942-4

[7] Yüzügüllü, O., Fajraoui, N., Liebisch, F. (2024). Soil texture and pH mapping using remote sensing and support sampling. IEEE Journal of Selected Topics in Applied Earth Observations and Remote Sensing, 17: 12685-12705. https://doi.org/10.1109/JSTARS.2024.3422494

[8] Zhang, H.M., Zhou, T., Geng, Y.J., et al. (2026). National-scale digital mapping of soil pH using Sentinel-2 optical data and multi-feature Sentinel-1 SAR data. Agriculture, 16(16): 1771. https://doi.org/10.3390/agriculture16161771

[9] Taqi, A.H., Al Nuaimy, Q.A.M., Karem, G.A. (2016). Study of the properties of soil in Kirkuk, IRAQ. Journal of Radiation Research and Applied Sciences, 9(3): 259-265. https://doi.org/10.1016/j.jrras.2016.02.006

[10] Terzi, M.A., Al Nuaimy, Q.A.M., Kadioğlu, Y.K. (2026). Evaluation of Sentinel-2 spectral indices for iron and aluminum mapping using integrated remote sensing and laboratory analysis: A case study in Kirkuk, Iraq. International Journal of Design and Nature and Ecodynamics, 21(9): 2621-2632. https://doi.org/10.18280/ijdne.210911

[11] Xia, C.Z., Zhang, Y. (2022). Comparison of the use of Landsat 8, Sentinel-2, and Gaofen-2 images for mapping soil pH in Dehui, northeastern China. Ecological Informatics, 70: 101705. https://doi.org/10.1016/j.ecoinf.2022.101705

[12] Jassim, S.Z., Goff, J.C. (2006). The Geology of Iraq (First ed.). DOLIN, s.r.o. https://www.geolsoc.org.uk/bookshop/products/the-geology-of-iraq.

[13] Obaid, A.K., Allen, M.B. (2017). Landscape maturity, fold growth sequence and structural style in the Kirkuk Embayment of the Zagros, northern Iraq. Tectonophysics, 717: 27-40. https://doi.org/10.1016/j.tecto.2017.07.006

[14] Abdulrahan, Z.O., Al Nuaimy, Q.A.M., Mezaal, M.R. (2025). Assessing water reduction dynamics in the Chai River, Dakuk, Iraq using remote sensing and GIS tools. Western European Journal of Modern Experiments and Scientific Methods, 3(1): 1-15. https://westerneuropeanstudies.com/index.php/1/article/view/1909.

[15] Harris, S.A. (1960). Saline soils in the Kirkuk Plain, northern Iraq. European Journal of Soil Science, 11(1): 114-130. https://doi.org/10.1111/j.1365-2389.1960.tb02208.x

[16] Koshnaw, R.I., Horton, B.K., Stockli, D.F., Barber, D.E., Tamar-Agha, M.Y., Kendall, J.J. (2017). Neogene shortening and exhumation of the Zagros fold-thrust belt and foreland basin in the Kurdistan region of northern Iraq. Tectonophysics, 694: 332-355. https://doi.org/10.1016/j.tecto.2016.11.016

[17] Sissakian, V.K., Fouad, S.F.A. (2015). Geological Map of Iraq, Scale 1: 1000 000, 4th Edition, 2012. Iraqi Bulletin of Geology and Mining, 11(1): 9-16. https://ibgm-iq.org/ibgm/index.php/ibgm/article/view/263.

[18] Stock, A. (2025). Choosing blocks for spatial cross-validation: Lessons from a marine remote sensing case study. Frontiers in Remote Sensing, 6: 1531097. https://doi.org/10.3389/frsen.2025.1531097

[19] Roberts, D.R., Bahn, V., Ciuti, S., et al. (2017). Cross-validation strategies for data with temporal, spatial, hierarchical, or phylogenetic structure. Ecography, 40(8): 913-929. https://doi.org/10.1111/ecog.02881

[20] van der Meer, F.D., van der Werff, H.M.A., van Ruitenbeek, F.J.A., et al. (2012). Multi- and hyperspectral geologic remote sensing: A review. International Journal of Applied Earth Observation and Geoinformation, 14(1): 112-128. https://doi.org/10.1016/j.jag.2011.08.002